Asymmetric Random Average Process: Aggregation and Fragmentation on Continuous State Space

Frank Zielen and Andreas Schadschneider

Institute for Theoretical Physics, University of Cologne, Germany

Abstract. A simple analytically treatable stochastic process on continuous state space, the asymmetric random average process, with a broad range of applications in traffic flow theory, internet modeling and granular media is presented. We concentrate mainly on the analysis of the basic properties of the model. The set of all exact mean field solutions is determined and we point out that it represents a class of very good approximants even for non-product-measure processes. Furthermore we study a truncated process that shows the occurence of a nonsymmetric ergodicity breaking in the thermodynamic limit. This interesting phenomenon shows similar properties as spontaneous symmetry breaking, but without any explicit symmetry.

1 Model

The asymmetric random average process (ARAP) [1,2] is defined on a one-dimensional periodic lattice with L sites. Each site i carries a non-negative continuous mass variable m_i. In every discrete time step $t \to t+1$ for each site a random number $r_i \in [0,1]$ is generated from a time-independent probability density function (pdf) ϕ, sometimes called fraction density, that may depend on the actual configuration $m=(m_1,\dots,m_L)$. So the universal form can be written as $\phi=\phi(r_1,\dots,m_1,\dots)$. The fraction r_i determines the amount of mass $r_i m_i$ transported from site i to site $i+1$. The transport is completely asymmetric, i.e. no mass is transported in the opposite direction $i+1 \to i$ and we obtain

$$m_i \to (1-r_i)m_i + r_{i-1}m_{i-1} \ . \tag{1}$$

These update rules correspond to a parallel time dynamics. Due to the conservation of the total mass $M=\sum_i m_i$ the density $\varrho = \frac{M}{L}$ is fixed.

We would like to add that this so called stick representation can easily be mapped onto a particle picture: by considering L particles on a ring of length $L\varrho$ and denoting their positions by x_i, both representations become equivalent by identifying the masses m_i as the headway of particles, i.e. $m_i = d(x_i, x_{i+1})$. Due to the fact that the pdf ϕ depends only on the particle distances m_i, the ARAP is closely related to the class of car-following models.

For both pictures the update procedure is visualized in fig. 1, but in the following we will work in the stick representation only.

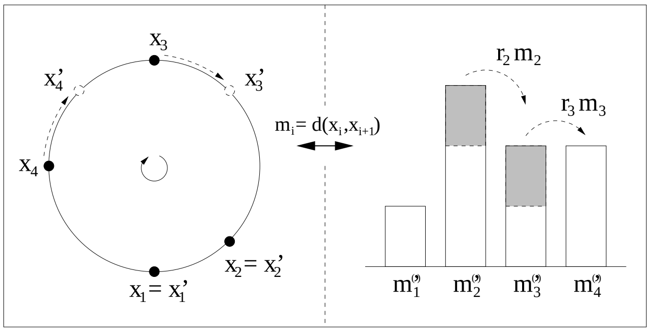

Fig. 1. Asymmetric Random Average Process: the random numbers r_i are generated according to a probability density $\phi = \phi(r_1, \ldots, m_1, \ldots)$. The state variables x_i, m_i and x'_i, m'_i correspond to the time t and $t+1$, respectively.

2 Fundamental Results

The basic quantity we are interested in is the mass pdf $P(m,t)$. The knowledge of this function corresponds to the complete solution of the problem. In the following we restrict our considerations to steady state dynamics only, i.e. the master equation

$$P(m'_2, \ldots, m'_k) = \int_0^\infty d^k m\ P(m) \int_0^1 d^k r\ \phi(r,m) \times \prod_{i=2}^{k} \delta\left(m'_i - [r_{i-1}m_{i-1} + (1-r_i)m_i]\right) \quad (2)$$

with $P(m) = \lim_{t\to\infty} P(m,t)$. Determination of a ($k$–1)-site mass distribution presumes the calculation of the k-site distribution. Thus we are confronted with a hierarchy of an infinite number of equations in the limit $L\to\infty$.

The simpliest version of the ARAP is obtained if we use the state independent uniform distribution defined by the fraction density $\phi = 1$. We will refer to this system as the free ARAP. Some results have been derived for this model so far whereby the exactness of product measure for $L\to\infty$ and its form [3]

$$P(m) = \prod_i P(m_i) \quad \text{with} \quad P(m_i) = \frac{4m_i}{\varrho^2}\, \mathrm{e}^{-2m_i/\varrho} \quad (3)$$

is an important one within the scope of this work. Equation (3) has been derived in the context of the q model [3] that has been developed for the description of force fluctuations in bead packs and shares many properties with the ARAP.

Another significant result is the factorization of the stationary two-point mass correlations for $\phi = \prod_i \phi(r_i)$, i.e. for ARAPs given by state and site independent pdfs [1]. This indicates that mean field calculations rather generally yield good approximations and that the class of exact mean field mass distributions represents an important subset of the solution space.

Further findings related to the ARAP, e.g. the consideration of other kind of updates, a discrete state space or symmetric mass movements, can be found in [2,4–6].

3 Exact Mean Field Solutions

In this section we determine all exact stationary mean field (MF) solutions for $\phi = \prod_i \phi(r_i)$ in the limit $L \to \infty$. This has been done explicitly in [6] and we would like to sketch the basic strategy here. Furthermore we show that our findings also represent very good approximants for arbitrary ϕ-functions.

Although the MF ansatz $P(m) = \prod_i P(m_i)$ decouples the infinite set of equations (2) we have to check consistency of (2) by inserting a MF solution into all equations. However, by k-dimensional Laplace transforming the k-site mass densities and introducing the functional map

$$F_Q(s,\tilde{s}) \equiv \int_0^1 dr\ \phi(r) Q\left((1-r)\,s + r\tilde{s}\right) \tag{4}$$

we reduce the infinite set of equations to the MF criterion (MFC)

$$F_Q(s_1,s_2) = F_Q(s_1,0) \cdot F_Q(0,s_2)\ . \tag{5}$$

For $s_1{=}s_2{=}s$, (5) acts as a conditional equation for the determination of a MF solution and yields

$$Q(s) = \int_0^1 dr\ \phi(r) Q(rs) \int_0^1 dr\ \phi(1-r) Q(rs)\ . \tag{6}$$

Putting (6) in (5) we can easily check the exactness of the MF solution. By expanding the single site Laplace transformed $Q(s)$ in a series around zero – this is always possible [6] – and representing the fraction density ϕ by its moments $\mu_n \equiv \int dr\ r^n \phi(r)$, the set $\mathcal{M}$ of all density functions ϕ resp. $\{\mu_n\}$ yielding exact MF solutions is calculated:

$$\mathcal{M} = \left\{ \{\mu_n\}_{n\in\mathbb{N}}\ \middle|\ \mu_n = \frac{\Gamma(n+\lambda_1)}{\Gamma(\lambda_1)} \frac{\Gamma(\lambda_2)}{\Gamma(n+\lambda_2)} \right\} \tag{7}$$

with

$$\lambda_1 = \mu_1 \frac{\mu_1 - \mu_2}{\mu_2 - \mu_1^2} \quad \text{and} \quad \lambda_2 = \frac{\mu_1 - \mu_2}{\mu_2 - \mu_1^2}\ . \tag{8}$$

So $\mathcal{M}$ is only parameterized by μ_1 and μ_2 that have to be chosen with respect to the general moment properties $1 > \mu_1 > \mu_2 \geqslant \mu_1^2$. We would like to note that the derivation of (7) is exact up to a conjecture which has been verified only partially until now [6].

The case $\mu_2 = \mu_1^2$, corresponding to $\phi(r) = \delta(r - \mu_1)$, is not covered by (8) and leads directly to $P(m) = \delta(m - \varrho)$. For $\mu_2 > \mu_1^2$ we are able to calculate the general form of the MF mass distributions and obtain

$$P(m) = \frac{\lambda_2^{\lambda_2}}{\Gamma(\lambda_2)} \frac{1}{\varrho} \left(\frac{m}{\varrho}\right)^{\lambda_2 - 1} \mathrm{e}^{-\lambda_2 \frac{m}{\varrho}} . \tag{9}$$

In contrast to (7) depending on both λ_1 and λ_2, $P(m)$ is a function of λ_2 only. So MF ARAPs with fixed λ_2 and arbitrary λ_1 have identical mass distributions.

For arbitrary ARAPs given by $\phi = \prod_i \phi(r_i)$ with $\phi \notin \mathcal{M}$ we are able to construct appropriate approximants with the help of (8) and (9). This is done by calculating the parameter λ_2 that determines the shape of $P(m)$ from the first and second moment μ_1 and μ_2 of ϕ and inserting this value in (9).

As an example we present the simplest version of an ARAP with truncation. It is based on the free ARAP but enhanced by an additional parameter $R \in (0, 1]$. The cutoff R controls the movement in the following way: A stick fragment $r_i m_i$ is only transferred if $r_i \leq R$. The corresponding density function takes the form

$$\phi_R(r) = (1 - R)\delta(r) + \theta(R - r) \tag{10}$$

where θ is the Heaviside step-function. One can easily prove that $\phi_R \notin \mathcal{M}$ for $R < 1$, so mean field is not exact. Nevertheless we obtain by the construction presented above approximants that match the Monte Carlo simulation data very well (see fig. 2a). Only for small masses m systematical differences occur.

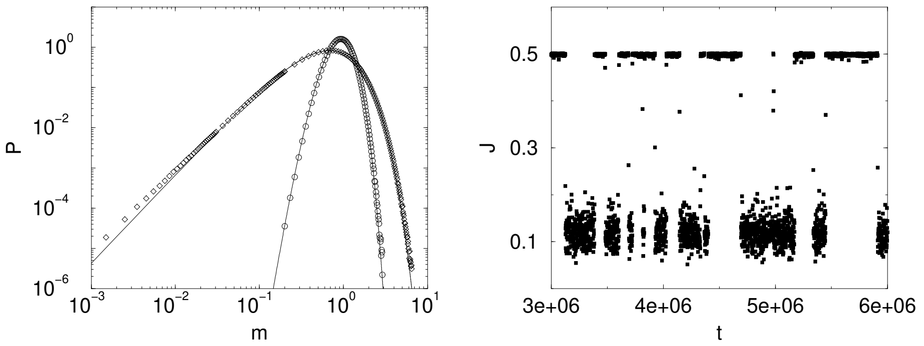

Fig. 2. (a) Analytical [–] and numerical [$R = 0.1(\circ), 0.5(\diamond)$] single site mass distributions of the truncated ARAP $\phi_R(r) = (1-R)\delta(r) + \theta(R-r)$. **(b)** Current-time diagram of the TARAP in the mixed phase ($L = 100$, $\tilde{\Delta} = 0.846$)

4 Nonsymmetric Ergodicity Breaking

In this section a truncated ARAP with site dependent fraction function of the form $\phi = \prod_i \phi(r_i, m_i)$ is presented. A phase characterized by the occurence of nonsymmetric ergodicity breaking is observed. In the following we summarize primarily the main results of [7].

The free ARAP is equipped with a simple additional update rule: transfers of masses $r_i m_i$ larger than a cutoff $\Delta > 0$ are rejected. This represents a truncated ARAP (TARAP) with fraction density

$$\phi(r,m) = [1 - R(m)]\,\delta(r) + \Theta\left(R(m) - r\right) \ , \tag{11a}$$

$$R(m) = \min\left(1, \Delta/m\right) \ . \tag{11b}$$

By substituting $m \to \varrho$ in (11b) we obtain the site independent fraction density (10) with $R = R(\varrho)$. We identify two phases in this toy model: For $\Delta \geqslant \varrho$ we obtain $\phi = 1$ and the system is exactly solved by (3). For $\Delta < \varrho$ we are in a phase described by the existence of truncation.

By restricting to the case $\varrho = 1$ (without loss of generality) and introducing the rescaled cutoff

$$\tilde{\Delta} \equiv 2L^{-\frac{1}{2}}\Delta \tag{12}$$

we also identify two phases in the TARAP. Our results base on Monte Carlo simulations and analytical approximations.

For $\tilde{\Delta} > \tilde{\Delta}_c \equiv 1$ the system remains in a high flow phase, i.e. the mass is distributed homogeneously and approximatively given by (3). The current, i.e. the average mass shift per site, is independent of the rescaled cutoff and equal to the flow of the free system ($J_{\text{high}} = J_{\text{high}}^{\max} \equiv \frac{1}{2}$).

For $\tilde{\Delta} < \tilde{\Delta}_c$ the TARAP is in a mixed phase. Here the system can either exist in a high flow state (with properties as described above) or a low flow state. The latter is given by an macroscopic condensate on one site which corresponds to a jam in the particle picture. Simulations have shown that configurations with two or more aggregates are not stable and merge into one column after a while. The flux of the low flow state is given by $J_{\text{low}} = J_{\text{low}}^{\max}(1 - (1 - \tilde{\Delta}^2)^{\frac{1}{2}})$ with $J_{\text{low}}^{\max} \equiv \frac{1}{4}$.

In finite systems the average lifetimes τ_{low}, τ_{high} of the low and high flow states are finite. So a single system switches between these states while evolving in time and an alternating current-time relation is obtained (fig. 2b).

In the thermodynamic limit simulations and analytical estimations indicate a diverging behaviour of the lifetimes, i.e. τ_{low}, $\tau_{\text{high}} \to \infty$ for $L \to \infty$. So ergodicity is broken because in dependence of the initial condition the system evolves into the high flow or the low flow state and will stay there forever. It is remarkable that low and high flow state are obviously not related by symmetry, so we call this effect a nonsymmetric ergodicity breaking.

We would like to remark that the scaling of the average lifetimes with the system size is different for high and low flow states. Although it is very difficult to fit the numerical curves appropriately τ_{low} seems to increase algebraically with L while the L-dependence of τ_{high} seems to be exponential. This behaviour reflects different switching mechanisms. The transition from the homogeneous high to the singular low flow state is mainly driven by fluctuations while the opposite transition is based on slow dynamics – it takes a long time to reduce an infinite aggregate.

5 Discussion

In this work the ARAP has been studied on a fundamental level. In section 3 exact solutions and approximations for state and site independent fraction densities $\phi = \prod_i \phi(r_i)$ have been derived. In section 4 we have provided evidence for an interesting new feature, nonsymmetric ergodicity breaking, which can be observed in the truncated variant of the ARAP.

However, if we try to model problems of traffic or granular flow in terms of the ARAP we will in general be confronted with more complicated fraction densities. But there are some questions that can be answered by the use of simple ARAPs, i.e. simple ϕ-functions. The q model [3] is a good example here. Furthermore the TARAP can be treated as a stochastic toy model of internet transport: a ring of routers $\{i\}$ with actual storage m_i shuffles data packages in a preferred direction. Multiple and uncorrelated requests are realized by transporting only random fractions $r_i m_i$ to the next neighbour and a maximum band width is represented by the cutoff Δ. Based on this model we are able to compute a quantity like $\tilde{\triangle}_c$ that reflects a critical band width considered as a lower bound for uncongested traffic. However, more realistic internet models must incorporate more features like bounded router capacities, open boundaries or re-sending processes.

So the ARAPs studied here fulfill mainly the role of toy models that give qualitative estimations, e.g. by the $m \to \varrho$ substitution for site dependent ϕ's, or explain physical effects of more complicated processes. As an example we would like to mention the Krauss model [8] for traffic flow that represents a continuous version of the Nagel-Schreckenberg model. This system shows a similiar phase coexistence like the TARAP in the mixed phase, but the underlying dynamics are complex which complicates an analytical treatment. On the other hand, the essentials supporting the occurence of the mixed phase are identical in both models: truncation on a continuous state space. So the TARAP might catch some of the fundamental physics behind the Krauss model.

References

1. Krug, J. and García, J., J. Stat. Phys. **99**, 31 (2000).
2. Rajesh, R. and Majumdar, Satya N., J. Stat. Phys. **99**, 943 (2000).
3. Coppersmith, S. N. *et al.*, Phys. Rev. E **53**, 4673 (1996).
4. G. M. Schütz, J. Stat. Phys. **99**, 1045 (2000).
5. Rajesh, R. and Majumdar, Satya N., Phys. Rev. E **64**, 036103 (2001).
6. Zielen, F. and Schadschneider, A., J. Stat. Phys. **106**, 173 (2002).
7. Zielen, F. and Schadschneider, A., in preparation.
8. Krauss, S., Wagner, P., and Gawron, C., Phys. Rev. E 3707 (1996).